Breakdown of the quantized Hall effect in the vicinity of current contacts

Y. Kawano and S. Komiyama
Department of Basic Science, University of Tokyo, Komaba 3-8-1, Meguro-ku, Tokyo 153-8902, Japan
(Received 20 May 1999)

Spatial distribution of the cyclotron radiation emitted from nonequilibrium electrons is studied on 1.5 mm-wide Hall bars in the quantized Hall effect (QHE) regime. At low-current levels where the two terminal resistance is quantized, the cyclotron emission (CE) is observed at the electron entry and exit corners formed between the metallic current contacts and the two-dimensional electron gas (2DEG) layer. As the current increases, additional CE occurs in the vicinity of the corner of the source contact that is opposite to the electron entry corner. The additional CE is accompanied by a finite voltage drop. The region over which the finite voltage drop takes place is localized to the limited region adjacent to the source contact where the CE is observed, and shows that the QHE breaks down locally in the vicinity of the source contact before the breakdown develops in the entire 2DEG channel. Studies of device-width dependence reveal that this local breakdown of the QHE in the vicinity of the source contact takes place only in sufficiently wide Hall bars (with a width well larger than 200 μm). All the experimentally observed features are reasonably interpreted by assuming that electron-hole pairs are generated in cascading process due to strong polarization fields formed along the interface between the metallic source contact and the 2DEG.

I. INTRODUCTION

The dissipationless state of two-dimensional electron gas (2DEG) systems in the regime of quantized Hall effects (QHE) breaks down as the current passing through a device exceeds a critical value.[1,2] Experimentally the breakdown phenomenon has been extensively studied on Hall bars, which have current contacts at which electrons enter and leave the 2DEG. Most of the experiments studied the four-terminal resistance, yielding experimental results similar to those obtained on Corbino discs without current contacts.[1,3,4] This indicates that the presence of current contacts in a Hall bar does not play an essential role for the breakdown in a region sufficiently far away from the current contacts (at a distance of more than a few hundred micrometers). It is also indicated that the breakdown occurs when the Hall electric field averaged in the 2DEG channel exceeds a critical value.

Apart from the QHE breakdown in the 2DEG channel mentioned in the above, a particular feature is expected in the close vicinity of metallic current contacts. When a finite voltage is applied to a QHE Hall bar, strong polarization fields are expected to develop at the interface between the metallic current contacts and the 2DEG layer.[5] The maximum amplitude of the field, $E_{contact}$, may be roughly estimated as V_{SD}/λ, where V_{SD} is the source-drain voltage and λ is the screening length of the 2DEG. The polarization fields along the contact boundaries are typically much larger than the average Hall electric field in the channel, $E_{channel} = V_{SD}/W$, where W is the width of the device. As the current increases, therefore, the breakdown of the QHE may initiate in the boundary regions of current contacts.

Very little is yet clarified experimentally about what indeed happens in the close vicinity of current contacts with increasing the current. Resistance measurements are made on wide GaAs Hall bars[6] as well as on relatively wide silicon metal-oxide-semiconductor (Si-MOS) Hall bars.[7] In both experiments finite voltage drop is reported to take place at lower currents in a region close to the current contacts. In the experiment of van Son and coworkers,[7] finite voltage drop occurs only in the vicinity of the (electron-injecting) source contact but not in the vicinity of the drain contact. The authors suggested that nonequilibrium electrons are generated in the close vicinity of the source contact due to tunneling injection into the 2DEG and it causes a finite voltage drop there. However, our recent experiments studying cyclotron radiation in wide GaAs Hall bars have revealed that although nonequilibrium electrons are indeed injected from the source contact they do not lead to finite voltage drop in the Hall bar and that nonequilibrium electrons are generated also in the vicinity of the drain contact.[8] Thus, the mechanism of finite voltage drop reported in the earlier experiments are left to be clarified, and its relationship to the local breakdown expected in the vicinity of current contacts, as suggested in the last paragraph, is unclear.

In general, breakdown phenomenon is accompanied by generation of nonequilibrium electrons. Conventional measurements of IV characteristics alone provide only a limited information about the spatial distribution of the nonequilibrium electrons. In contrast, cyclotron radiation associated with the inter-Landau-level electron transition provides us with an experimental tool for directly probing the nonequilibrium electrons. In this paper, we carry out spatially resolved measurements of cyclotron emission (CE) from wide GaAs Hall bars along with the standard IV characteristic measurements.

We find that CE occurs in a region adjacent to the source contact when the current reaches a threshold value much smaller than the critical value for the QHE breakdown in the entire 2DEG channel. Coincidentally to this CE, finite voltage drop emerges in the relevant region, indicating that the local breakdown of the QHE takes place as expected in the above. The local breakdown, however, does not take place in the vicinity of the drain contact. We also find that the local breakdown near the source contact occurs only in sufficiently wide Hall bars ($W > 200$ μm). We will interpret these ex-

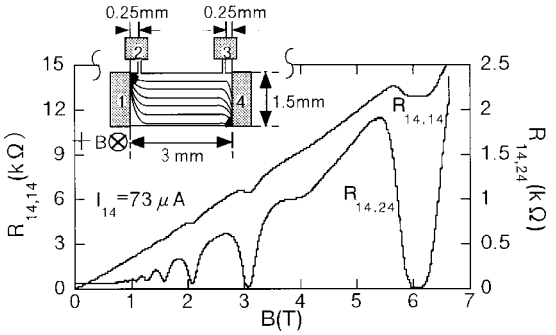

FIG. 1. The two-terminal resistance $R_{2t}=R_{14,14}$ and the three-terminal resistance $R_{3t}=R_{14,24}$ as a function of magnetic field at $I_{14}=73$ μA. The inset illustrates the sample.

perimentally observed features in terms of the bootstrap-type electron heating[9–13] (BSEH) induced by strong polarization fields distributed along the boundary of current contacts.

II. EXPERIMENTAL METHODS

The sample is a 3mm-long and 1.5 mm-wide Hall-bar as depicted in the inset of Fig. 1, which is fabricated on a GaAs/Al_xGa_{1-x}As heterostructure crystal with a 4.2 K mobility of 80 m^2/Vs and a 4.2 K-electron density of 2.6 $\times 10^{15}/m^2$. The CE is studied by using a high-sensitive photoconductive detector based on the cyclotron resonance of a high-mobility 2DEG in GaAs/Al_xGa_{1-x}As heterostructures.[14,15] The detector is fabricated on the same GaAs/Al_xGa_{1-x}As heterostructure crystal as that used for the sample. The spectral response of the detector has been studied by using a Fourier transform spectrometer, and shown to be due to sharp cyclotron resonance of the 2DEG with a full width at half maximum of about 1.5 cm^{-1} in the range of magnetic fields studied. The relationship between the detected wavelength and the applied magnetic fields is determined through the Fourier transform spectroscopy.

The experimental setup and the measurement method are similar to those applied in our previous work.[8] The sample and the detector are separated at a distance of about 29 cm, and placed, respectively, at the centers of two superconducting solenoids installed in a liquid Helium cryostat. The sample is excited with low-frequency square waves of current (20 Hz), alternating between zero and a defined value, and the modulation signals are detected with a lock-in amplifier. For spatially resolved measurements of CE, the sample is moved by using a mechanical $X-Y$ translation stage. The far infrared radiation is collected by a convex lens and guided to the detector through a light pipe. Below we denote by $R_{ij,kl}$ the resistance V_{kl}/I_{ij} obtained when the voltage V_{kl} is measured between contacts k and l where the current I_{ij} is transmitted from contact i to contact j. Throughout this paper, the polarity of current is defined as positive when the electrons enter the 2DEG from contact 4 and leave for contact 1. All the measurements are carried out at 4.2 K.

III. EXPERIMENTAL RESULTS

A. Cyclotron emission

Figure 1 illustrates the two-terminal resistance $R_{14,14}$ and the three-terminal resistance $R_{14,24}$ as a function of magnetic field B at $I_{14}=+73$ μA, and demonstrates the quantization of $R_{14,14}=h/2e^2$ and the vanishing of $R_{14,24}$ in the QHE states of $\nu=2(B\sim 6$ T) and $\nu=4(B\sim 3$ T).

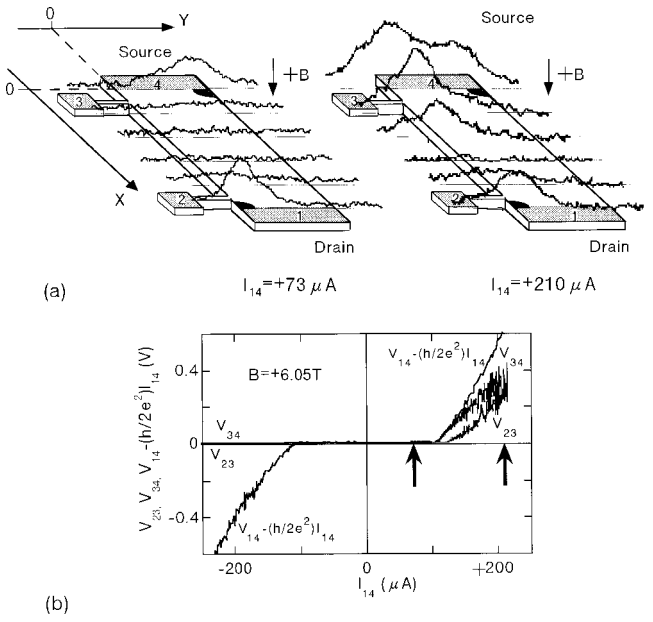

FIG. 2. (a) The spatial distribution of CE at $I_{14}=+73$ μA (left panel) and at $I_{14}=+210$ μA (right panel) for $+B$. Black shadings mark the electron entry and exit corners. (b) Voltages V_{23}, V_{34}, and $V_{14}-h/2e^2$ versus current I_{14}. Two arrows mark the two current values, at which the CE's in (a) are studied.

CE is studied in the QHE state of $\nu=2(B=6.05$ T). The magnetic field for the detector is fixed at $B_D=5.99$ T. Figure 2(a) displays the spatial distribution of CE intensity for the two different currents, $I_{14}=+73$ μA and $+210$ μA. The spatial resolution of the measurement system is about 0.3 mm. The data are taken by moving the sample along the width-wise direction (Y), while the position in the length-wise direction (X) is shifted at a step of 0.6 mm for each emission line. The spectrum of emission will be described in Sec. IIID. The left panel of Fig. 2(a) is for $I_{14}=+73$ μA and shows that the region of CE is restricted to the vicinity of the current entry and exit corners of the Hall bar as marked by black shadings. These emissions occur without causing a longitudinal resistance or an excess contact resistance as seen from the vanishing of $R_{14,24}$ and the quantization of $R_{14,14}$ in Fig. 1. In our previous work, we have found that these emissions are observable even at much lower currents, and interpreted them as arising from the local nonequilibrium population of electrons intrinsically induced by the strong polarization fields concentrated at these electron entry and exit corners.[8]

As the current increases above 100 μA, an additional region of CE develops only on the side of the (electron-injecting) source contact as shown for $I_{14}=+210$ μA in the right panel of Fig. 2(a). (Compared to the data in the left panel, the curves are drawn with a reduced scale by a factor 1/5.) Differently from the CE occurring at smaller currents, this additional CE gives rise to a finite longitudinal resistance. The voltages V_{34}, V_{23}, and V_{14} are displayed against I_{14} in Fig. 2(b), where V_{14} is represented by the difference from the quantized value, $V_{14}-(h/2e^2)I_{14}$.

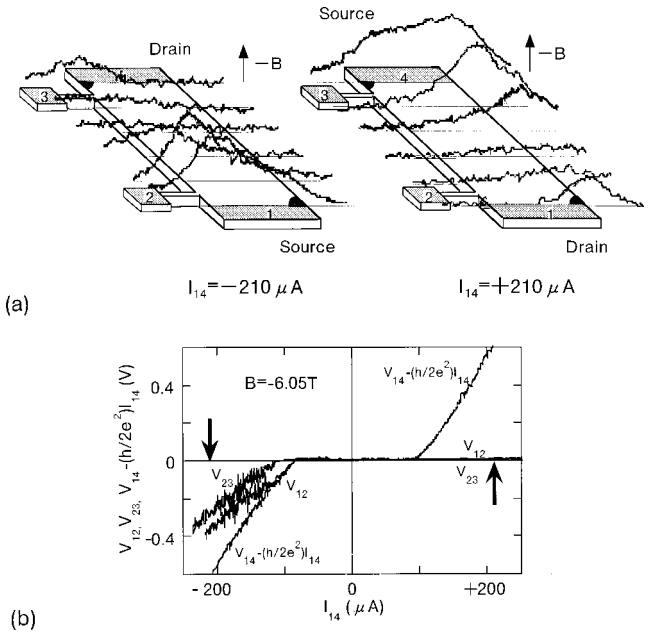

FIG. 3. (a) The spatial distribution of CE at $I_{14}=-210\ \mu$A (left panel) and at $I_{14}=+210\ \mu$A (right panel) for $-B$. Black shadings mark the electron entry and exit corners. (b) Voltage V_{12}, V_{23}, and $V_{14}-h/2e^2$ versus current I_{14}. Two arrows mark the two current values, $I_{14}=-210\ \mu$A and $I_{14}=+210\ \mu$A, at which the CE's in (a) are studied.

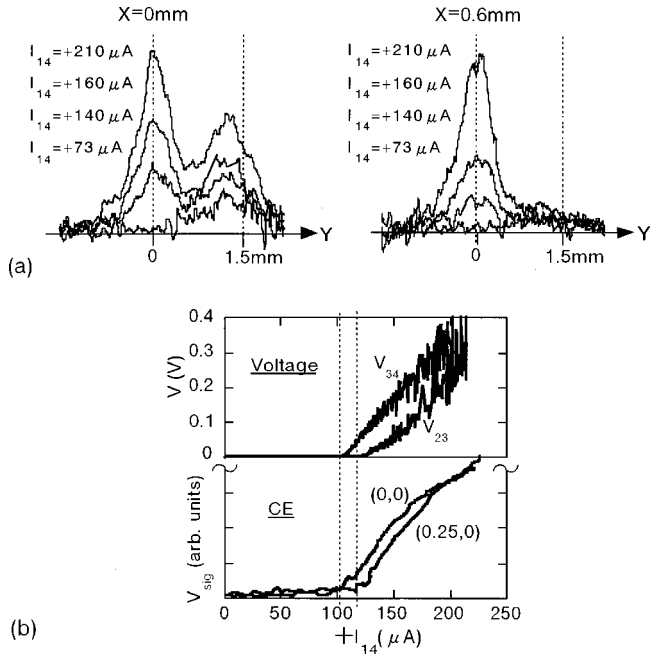

FIG. 4. (a) Intensity profile of the cyclotron emission along the boundaries at $X=0$ mm (left panel) and $X=0.6$ mm (right panel) for $+B$. The dotted lines, marking the positions of $Y=0$ mm and 1.5 mm, indicate the width of the Hall bar. (b) The upper panel displays V_{23} and V_{34} against I_{14}. The lower panel shows the intensity of CE against I_{14} at two positions $(X,Y)=(0,0)$ and $(0.25,0)$. The polarity of B is positive.

Let us first pay attention to the behavior of these voltages for the positive polarity of currents. The two arrows in Fig. 2(b) mark the two current values, at which the CE's for Fig. 2(a) are studied. We note that both V_{34} and V_{23} become finite and V_{14} deviates from the quantized value when I_{14} exceeds about $+100\ \mu$A. The voltage drop takes place primarily along the sample boundary between contacts 4 and 3, and also occurs along the boundary between contacts 3 and 2. We find that the equality $V_{23}+V_{34}=V_{14}-(h/2e^2)I_{14}$ holds accurately in the range of larger currents $I_{14}>+100\ \mu$A.[16] Therefore, voltage drop (except the quantized Hall voltage) does not take place between contacts 2 and 1. Thus, it is suggested that the region of the finite voltage drop agrees with that of the additional CE. The features of the CE along with the IV-characteristics described in the above change systematically upon reversal of the polarity of magnetic field $(-B)$ as shown in Figs. 3(a) and 3(b), indicating that these features are intrinsic to the Hall bar.

Striking correlation between the additional CE and the voltage distribution in the vicinity of source contact is clarified in a more straightforward manner in Figs. 4(a) and 4(b). The development of the CE with increasing I_{14} for the positive polarity of magnetic field is elucidated in Fig. 4(a). Here the left panel displays the profile of the CE intensity along the boundary between contact 4 and the 2DEG layer, $X=0$ mm, and shows that the CE rapidly develops to form an additional prominent peak at the corner, $(X,Y)=(0,0)$, opposite to the electron-entry corner, $(X,Y)=(0,1.5$ mm). We note that, as a whole, the CE peak that was present at (0, 1.5 mm) already with lower currents does not exhibit peculiar dependence on I_{14} except that the intensity smoothly increases with I_{14}. However, we can also note that the profile of the CE at 73 μA has a weak longer tail towards the opposite corner, (0,0). [Compare the corresponding profile at the drain contact shown in the left panel of Fig. 2(a). The systematical difference is noted between the source and the drain contacts in the opposite polarities of currents and magnetic fields[8]]. This suggests that the region of nonequilibrium electron distribution expands along the boundary of the source contact towards the corner, (0,0), already at the current of 73 μA, and that the prominent peak of CE rapidly develops at the corner, (0,0), when the region reaches there. These features will be reasonably interpreted in Sec. IV.

The right panel of Fig. 4(a) displays the profile along the line crossing the 2DEG layer at $X=600\ \mu$m, and shows that the region of the additional CE extends along the boundary of the 2DEG, $Y=0\ \mu$m.

The lower panel of Fig. 4(b) shows the CE intensity as a function of $+I_{14}$ at corner (0,0) and at position (0.25 mm,0), at which the probe arm of contact 3 is attached. The CE's at these positions correlate, respectively, with the curves of V_{34} and V_{23} shown in the upper panel of Fig. 4(b), where the data of Fig. 2(b) are replotted. Namely, the CE at the corner of (0,0) occurs at about $I_{14}=+100\ \mu$A and it coincides with the occurrence of finite voltage drop in V_{34}, and the CE at the position of contact 3, $(0.25\,\text{mm},0)$, occurs at about $I_{14}=+120\ \mu$A and it coincides with the occurrence of voltage V_{23}. The coincidence definitely indicates that the region of the additional CE along the boundary of the 2DEG layer is identical to the region of the finite voltage drop and that the region expands along the boundary as I_{14} increases. We note that the relevant boundary is the higher-energy edge (for electrons) of the Hall bar.

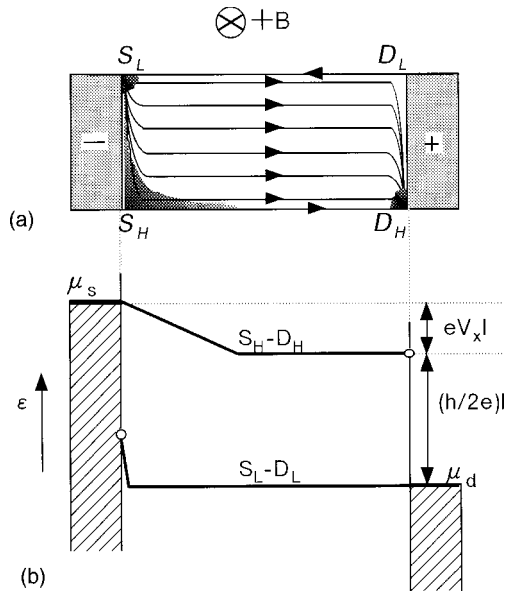

FIG. 5. (a) Schematic representation of the sample along with the regions of CE observed at $I>100$ μA. The arrows indicate the direction of electron propagation. (b) Schematic representation of the electrochemical potential along the boundaries $S_H-(D_H)$ and $(S_L)-D_L$ in the condition illustrated in (a).

Let us consider the lower-energy edge of the Hall bar for completeness of discussion. For this sake, we pay attention to the negative polarity of current in Fig. 2(b), where contact 1 serves as the source of electrons. The boundary of the Hall bar on which voltage probes 3 and 4 are attached corresponds now to the lower-energy edge. Differently from the case of positive currents, the voltages V_{23} and V_{34} remain vanishing in the entire range, yielding highly asymmetric IV-characteristics about $I_{14}=0$. In contrast, V_{14} shows, of course, the anti-symmetric IV-characteristics about $I_{14}=0$. This indicates that the excess longitudinal voltage that causes V_{14} to deviate from $h/2e^2$ is restricted to the region between contacts 2 and 1 for the negative polarity of current. We also mention that this voltage drop must occur coincidentally with the voltage drop along the higher-energy edge (between contacts 4 and 3). Note also that the feature changes systematically upon reversal of the polarity of magnetic field [Fig. 3(b)].

Figures 5(a) and 5(b) summarize the findings obtained in the above. At low currents below 73 μA, the CE is visible only in the vicinity of the electron entry and exit corners, marked, respectively, by S_L and D_H in the Hall bar schematically shown in Fig. 5(a). Except the Hall voltage, no appreciable voltage drop occurs along the boundaries of the 2DEG. Namely, the electrochemical potentials along the higher-energy boundary $S_H-(D_H)$ and the lower-energy boundary $D_L-(S_L)$ are constants and are, respectively, equal to the those of the source and drain contacts, μ_S and μ_D. As the current increases to exceed about 100 μA, the additional CE appears at the corner S_H opposite to the electron entry corner, S_L, and expands along the higher-energy boundary S_H-D_H with further increasing the current, while the CE's at corners S_L and D_H survive without showing significant change in their profile. The occurrence of the additional CE at corner S_H and along the boundary S_H-D_H is accompanied by a longitudinal voltage drop along the relevant boundary. The region of the finite voltage drop is identical to the region where the additional CE occurs as schematically described in Fig. 5(b). Along the lower-energy boundary, D_L-S_L, the region of the finite voltage drop is localized in the close vicinity of corner S_L as indicated also in Fig. 5(b). On the side of the drain contact, neither additional CE nor anomalous voltage drop appears.

The critical current $I_{14}=100$ μA, at which the finite volatge drop emerges in the region adjacent to the source contact, is much smaller than the critical current expected for the QHE breakdown in the entire 2DEG channel of this wide Hall bar, $I=480$ μA.[10] This local breakdown phenomenon should be distinguished from another type of the QHE breakdown reported by Balaban and coworkers.[17] In the latter, the critical current increases sublinearly with the device width but the breakdown phenomenon occurs in the 2DEG region well away from the current contacts.

B. Device-width dependence

The occurrence of the additional CE and the relevant voltage drop are tightly linked to each other. Therefore, we may investigate the voltage drop instead of probing the CE. Asymmetric IV characteristics similar to those described in the above have been reported on GaAs Hall bars[6] as well as on Si-MOS Hall bars.[7] The characteristics are therefore supposed to be general for QHE Hall bars. However, it is important to note that all the Hall bars used in these works (including the present work) are relatively large, with a device width larger than about 200 μm. To our knowledge, the asymmetric IV characteristics as described in the above have never been reported on the devices of a width smaller than 100 μm. To specifically examine the device-width dependence, we have fabricated differently wide Hall bars on the same GaAs/Al_xGa_{1-x}As heterostructure crystal as that used in the present experiments, and studied the three terminal resistance. Figure 6 compares the curves of V_{24} versus I_{14} studied in the Hall bars of $W=1500$, 180, and 2 μm at $\nu=2$.

Note that V_{24} with the given polarity of magnetic field probes the voltage drop at the source contact for the positive polarity of current, and that at the drain contact for the negative polarity of current. In all the devices, the two-terminal voltage V_{14} is confirmed to show a regular antisymmetric behavior about $I_{14}=0$. It is clearly noted that the asymmetric feature of the V_{24} versus I_{14} curve is remarkable in the device of $W=1500$ μm but is much weaker in the device of $W=180$ μm. In the narrowest device of $W=2$ μm, the asymmetry vanishes completely. Although we do not show here, we have separately measured V_{23} and V_{34} in the opposite polarity of magnetic field, and confirmed that the asymmetry of the IV characteristics is caused by the voltage drop in the vicinity of the source contact as described already, and that the anomalous voltage drop relevant to the source contact vanishes as the device width decreases. We note again that this W dependence is different from the sublinear W dependence of the critical current for the QHE breakdown.[17]

C. Efficiency of energy conversion to the CE

When current I is passed through a Hall bar, the electric power of $V_{2t}I=(V_H+V_x)I$ is fed to the sample, where V_{2t} is

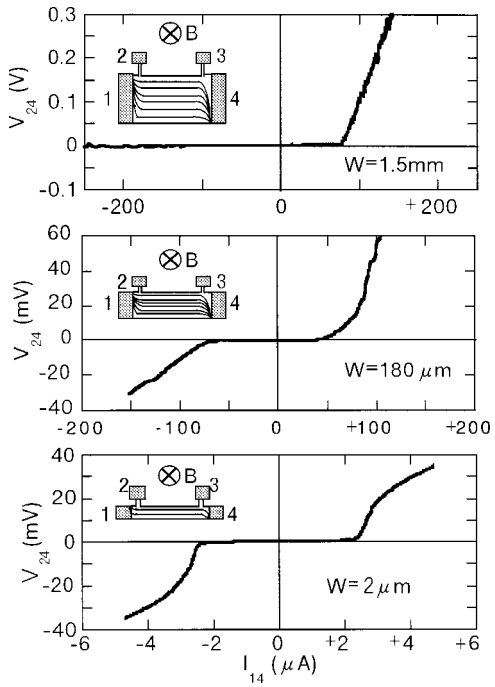

FIG. 6. Three-terminal voltage V_{24} as a function of current I_{14} in three differently-wide Hall bars.

the two-terminal voltage, $V_H=(h/2e^2)I$ is the quantized Hall voltage and V_x is the excess voltage drop in the Hall bar. The CE at corners S_L and D_H originates from the Hall voltage term, V_HI, while the additional CE at corner S_H and along the adjacent boundary S_H-D_H arises from the longitudinal voltage term V_xI. Therefore, we can define the efficiency of energy conversion into the respective CE's by dividing the integrated CE intensities by V_HI and V_xI, respectively. The conversion efficiency for the CE's at corners, S_L and D_H, has been estimated to be on the order of 10^{-6} at $I=100$ μA.[8] We note in the right panel of Fig. 2(a) that the integrated intensity of the CE at corner S_H and along the adjacent boundary S_H-D_L is roughly two times larger than that of the CE's at corners S_L and D_H. We also note in Fig. 2(b) that $V_x=V_{2t}-(h/2e^2)I$ is smaller than $V_H=(h/2e^2)I$ by a factor about 4.5 at $I=210$ μA. Hence, we estimate the efficiency of energy conversion for the additional CE to be about ten times larger than that for the CE's at corners S_L and D_H at $I=210$ μA. This marked difference suggests difference in the mechanism between these CE's.

D. Cyclotron effective mass

The spectrum of CE has been studied separately for the regions of S_L,D_H, and S_H. The three panels of Fig. 7 display, respectively, the spectra at corners S_L,D_H and S_H from the top for the currents of 200 and 550 μA. In each panel, the CE intensity measured with the detector in a fixed magnetic field of $B_D=5.99$ T is shown as a function of magnetic field B. The amplitude of each CE line is normalized for clarity. At currents lower than 80 μA, values of the cyclotron effective mass m_c^* corresponding to the CE is substantially the same between corners S_L and D_H and is given by $m_c^*=(0.069\pm0.0007)m_0$ with the free electron mass m_0, as we have reported in our previous work on the same sample.[8] This feature is kept unchanged when the current increases to 200 μA. The spectrum of additional CE, which appears at corner S_H as the current exceeds about 100 μA, corresponds also to the same cyclotron mass value and does not shift appreciably with further increasing the current as seen in the bottom panel of Fig. 6. With increasing the current to 550 μA, only the spectrum at corner D_H shifts to a higher B position (or a larger value of m_c^*) by about 1% as seen in the middle panel of Fig. 6.

The value of m_c^* associated with the transition between the lowest two bulk Landau levels ($\nu=2\rightarrow\nu=1$) is expected to be $m_c^*=(0.069\pm0.0003)m_0$ for this 2DEG system.[18] The conduction band nonparabolicity of GaAs predicts m_c^* to increase by $\Delta m_c^*/m_c^*=3.6\%$ and 7.2%, respectively, for the higher-level transitions $\nu=3\rightarrow2$ and $4\rightarrow3$.[19] If such higher-level transitions are involved in the present experiments, they would be resolved as additional shoulders in the line shape. This makes us to conclude that only the lowest transition, $\nu=2\rightarrow1$, is relevant in all the CE's observed. This suggests that the ''effective electron temperature T_e'' of the relevant nonequilibrium electron distribution is much less than the Landau level energy spacing, $\hbar\omega_c$. We have expected $T_e\approx10$–15 K for the CE's at corners S_L and D_H.[8] This also applies to the additional CE at corner S_H as will be discussed later.

The value of m_c^* may be also affected if the electrostatic potential in the region of the CE is distorted to yield a second derivative, $U''(x)$; viz., $\Delta m_c^*/m_c^*=\{1+(U''/\omega_c^2m_c^*)\}^{-1/2}-1$. The observed increase of m_c^* for the CE at corner D_H with increasing the current to 550 μA might suggest that the second derivative of potential, $U''(x)$, is negative and its amplitude increases with increasing the current at this corner. This is in qualitative agreement with the expected feature of the electrostatic potential at this corner.

IV. DISCUSSION AND INTERPRETATION

Before discussing the mechanism of the local breakdown of the QHE we need to briefly review the mechanism of the CE's occuring with smaller currents at corners S_L and D_H.[8] On application of a finite source drain voltage V_{SD}, a strong polarization field develops at the electron entry and exit corners, S_L and D_H. The amplitude of the field, being roughly estimated by $E_{contact}=V_{SD}/\lambda$, reaches as large as 100 kV/m$\sim$1000 kV/m at $I=10$ μA if we assume $\lambda=0.1\sim1$ μm. At relatively low currents, therefore, the plarization fields at corners S_L and D_H are already strong enough to cause tunneling of electrons between the electron reservoirs (in the contacts) and Landau levels (in the 2DEG) and between Landau levels. As discussed earlier,[8] these tunnelling processes lead to generation of nonequilibrium electrons and the CE's at these corners. Importantly, however, these corners, S_L and D_H, are spatially separated, respectively, from the corners, S_H and D_L, through which electrons are respectively supplied into the edge states. Accordingly, the nonequilibrium electron distributions at these corners do not affect the population of edge states, and finite longitudinal voltage drop does not take place anywhere in the Hall bar (except the Hall voltage) despite these nonequilibrium electrons.

We now discuss the CE in the vicinity of corner S_H and consider the mechanism of the local breakdown of the QHE. In order to achieve satisfactory understanding, we need to clarify not only the mechanism but also the reason why it is absent on the side of drain contact and why it is totally absent in less-wide Hall bars. For this purpose, let us first note that, if the longitudinal resistivity is vanishing in the 2DEG, strong polarization field should develop not only at the corners but also along the boundary S_L-S_H (or D_L-D_H), where the field is expected to decrease from corner $S_L(D_H)$ towards $S_H(D_L)$. Consider first the kinetics of electrons on the side of source contact. Most of the electrons, except those entering the edge states from corner S_H, enter the 2DEG at corner S_L, and move along the boundary, S_L-S_H, towards the opposite corner S_H.[20,21] One might readily expect that the strong polarization fields distributed along the boundary, S_L-S_H, cause the QHE to break down and generate nonequilibrium electrons along the boundary. This idea is not sufficient by itself for the following reasons. First, the CE does not develop remarkably at corner S_L with increasing the current although the polarization field is strongest there: The additional strongest CE is visible in the vicinity of S_H, where the polarization field is lowest along the boundary, S_L-S_H. Second, it is expected that equally strong polarization fields are distributed along the boundary D_L-D_H but the corresponding CE is not observed experimentally. Third, the device-width dependence of the local breakdown is not explained.

The characteristics of the QHE breakdown found for long Hall bars[10–13,22] give important hints for understanding the local breakdown phenomenon. The most important feature is that the QHE breaks down at a critical electric field $E_c(5-30$ kV/m) that is much lower than the field value necessary for causing significant excitation of electrons to higher Landau levels through Zener-type tunneling[23]. The breakdown phenomenon occurs as an avalanche multiplication of excited electron-hole pairs during the drift of electrons along the Hall current, referred to as the BSEH.[10–13] The cascade excitation of electron-hole pairs is a relatively slow process. Therefore, in order for the longitudinal resistivity to appreciably increase in a given region, electrons reaching the region have to travel a sufficiently long distance. Therefore, electric fields higher than E_c have to be distributed over a macroscopic length along the trajectories followed by the electrons. The characteristic distance L_B needed for sufficient cascading is expected to be infinitely long at E_c and decrease with increasing the field beyond E_c. According to the experiments made at $B=6$ T ($\nu=2$) for the 2DEG in the same crystal as the one used in this work, L_B reaches more than a few hundred micrometers at an electric field by about 10% larger than the critical field $E_c\approx 20$ kV/m.[10,12] L_B is found to be not much smaller than 100 μm even for electric fields much larger than E_c. It is expected, and observed by experiments, that the minimal L_B (in the limit of strong fields) remarkably increases with increasing the magnetic field and with increasing the electron mobility.[10,12,13]

We interpret below the local breakdown of QHE in the light of the knowledge above. We first consider a wide Hall bar. As the current increases from zero, the polarization fields distributed along the boundary S_L-S_H will increase from zero. Consider the averaged field over the minimal length L_B, say 100 μm, along the boundary in the vicinity of corner S_L. It is important that the average field reaches the threshold value E_c for the BSEH already before Echannel reaches E_c. The inter-Landau-level (direct) excitation in this region remains unimportant. As the current increases, the region of the boundary along which the average field exceeds E_c will expand towards corner S_H. Hence, generation of electron-hole pairs will take place in this region, which yields CE along the boundary that expands its region towards corner S_H. However, the polarization fields can be high *only if the longitudinal resistivity is strictly vanishing* along the boundary: It is expected that the fields (except at corner S_L) are significantly reduced as the longitudinal resistivity increases. Thus, if the longitudinal resistivity is vanishing, the cascading multiplication of electron-hole pairs may develop, but if the cascade develops the polarization fields will be thereby strongly suppressed. Hence, we may assume that the polarization fields in the relevant region adjust themselves to be nearly equal to E_c. It follows that the generation of electron-hole pairs may be suppressed to a minimal level, leading to only a weak CE along boundary S_L-S_H. This explains the presence of a weak tail of the CE observed at 73 μA shown in the left panels of Figs. 2(a) and 4(a). Furthermore, the generated electon-hole pairs do not yield finite voltage drop unless the relevant region reaches corner S_H for the reason already mentioned in the above.

With increasing the current further, the region where $E\sim E_c$ will eventually reach corner S_H. At this point, the cascading generation of electron-hole pairs becomes possible over the entire boundary, S_L-S_H. The polarization fields distributed along the boundary adjust themselves similarly as in the above, but the self-consistent field (averaged over the boundary) can now increase above E_c as the current increases beyond this critical value. It follows that the significant population of electron-hole pairs can build up at the terminal of the cascade, that is, at corner S_H. Above this critical current, therefore, strong CE starts to develop at corner S_H. Coincidentally, finite voltage drop emerges in the relevant region, because the nonequilibrium distribution of electrons at corner S_H affects the population of the edge state (S_H-D_H), and causes the electrochemical potential along the edge state to decrease as the distance from corner S_H increases. This accounts for the observed features of the local breakdown of the QHE in the vicinity of the source contact. After reaching corner S_H, electrons will move away from the corner along the edge S_H-D_H, where the Hall electric field is lower than E_c. The population of the excited electron-hole pairs, therefore, decays as electrons move away from corner S_H along the edge S_H-D_H, where the decay rate will be slower as the current increases and the Hall electric field distributed along the edge approaches E_c. This expains the spatial profile of the CE in the vicinity of corner S_H shown in the right panel of Figs. 2(a), 3(a), and 4(a). The ''effective electron temperature T_e'' characterizing the nonequilibrium electron distribution has been estimated to be $kT_e=\hbar\omega_c/7$,[13] which is consistent with the observed value of the cyclotron mass of the CE.

Let us discuss the phenomenon on the side of drain contact. Similar arguments to the above applies to boundary D_L-D_H as well: If the current is large enough, cascade gen-

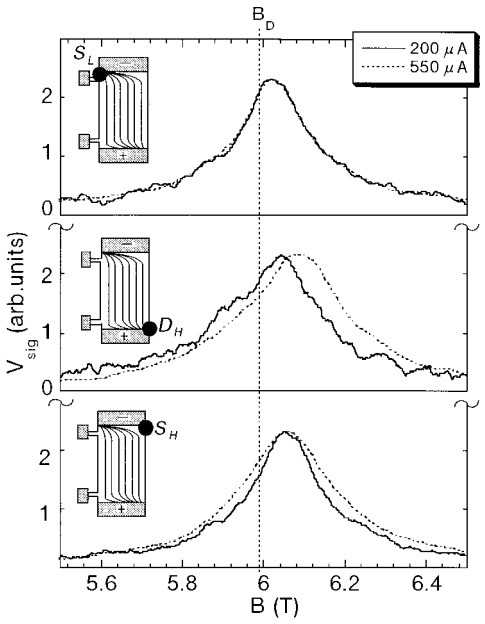

FIG. 7. Spectra of the cyclotron emission obtained at three different positions: S_L (the top panel), D_H (the middle panel) and S_H (bottom panel). The current is $I_{14}=200$ μA (solid lines) and 550 μA (dotted lines). The dashed line mark the magnetic field, $B_D = 5.99$ T, applied to the detector.

eration of electron-hole pairs may take place as electrons drift along the boundary from D_L towards D_H. However, since the terminal of the cascade stream is corner D_H, significant population of electron-hole pairs is expected to build up not at corner D_L but at corner D_H. Therefore, CE is not expected at corner D_L. We suppose further that the cascading-process-induced nonequilibrium electron distribution at corner D_H does not lead to strong CE for the following two reasons. First, the polarization field is very high at this corner. This will make the cyclotron radiation a less probable mechanism, compared to nonradiative processes like phonon emissions, as the channel of energy dissipation. This view is supported by the large difference in the efficiency of energy conversion between the CE's at corners S_H and $D_H(S_L)$, as discussed in Sec. IIIC. Secondly, the electron-hole pairs at corner D_H are absorbed by the drain contact immediately after they have built up. This prevents the electron-hole pairs from effectively contributing to the CE.

The nonequilibrium electron distribution at corner D_H does not affect the population of edge state for the reason mentioned in the above already, and therefore it does not lead to finite voltage drop. Thus, the local breakdown is not expected to take place on the side of drain contact.

All the experimentally observed features of the local breakdown of the QHE are thus explained by considering a cascadelike generation of electron-hole pairs due to BSEH.

Finally, let us consider the influence of the width, W, of the Hall bar on the local breakdown. It is generally expected that the polarization field at corner S_H is larger than the average Hall electric field in the 2DEG channel in standard Hall bars. Therefore, regardless of W, the polarization field is expected to reach E_c before the breakdown develops in the entire 2DEG channel. However this is not sufficient for the occurrence of the local breakdown. That is, W has to be larger than the minimal distance, L_B, needed for the cascading generation of electron-hole pairs to significantly develop, which is on the order of 100 μm in high- mobility GaAs systems. We expect that this is the reason why the local breakdown is absent in less-wide Hall bars.

If W is smaller than the minimal length, L_B, substantial population of nonequilibrium electrons will not build up at corner S_H even at very high currents, and the breakdown of the QHE in the 2DEG channel will not be preceded by the local breakdown in the vicinity of the contact. In such a Hall bar, cascadelike electron-hole pair excitation can take place only as the electrons traverse the Hall bar along the lengthwise direction of the 2DEG channel. The evolution of the breakdown is such that it initiates on the source-contact side of the 2DEG channel and develops towards the drain-contact side. Such a spatial evolution has been indeed observed by experiments for narrow Hall bars.[10–12,22]

If W is larger than a minimal length L_B as in the present experiments, the breakdown of the QHE in the entire 2DEG channel is necessarily preceded by the local breakdown around the source contact. As the current increases, the local breakdown will evolve continuously to the complete breakdown in the entire 2DEG channel.

V. CONCLUSION

We have visualized spacial distribition of nonequilibrium electrons excited in a 1.5 mm-wide Hall bar at different current levels by using the CE as a probe. As the current increases, finite voltage drop occurs locally in a region adjacent to the (electron injecting) source contact before the QHE breaks down in the entire 2DEG channel. Strong CE takes place coincidentally to the occurrence of finite voltage drop. Such a feature of the local breakdown of the QHE is not observed in the region adjacent to the drain contact. Additional studies of device-width dependence show that this local breakdown of the QHE in the vicinity of the source contact takes place only if the width of the Hall bar is sufficiently large (typically larger than 200 μm). All the experimentally observed features have been reasonably interpreted by assuming that electron-hole pairs are generated in a cascading process due to strong polarization fields formed along the interface between the metallic source contact and the 2DEG.

A consistent scenario has been thereby derived for the local breakdown of the QHE. In any Hall bars, generation of electron-hole pairs can initiate at the electron entry corner and it can develop along the boundary between the source contact and the 2DEG. If the width of a given Hall bar, W, is larger than the minimal distance L_B necessary for the cascading process of electron-hole pair generation to sufficiently develop, appreciable population of electron-hole pairs can build up as the electrons drift along the boundary. As the current increases in such Hall bars, finite voltage drop abruptly occurs when electron-hole pairs are excited along the entire boundary. As the current increases further, the region of the local breakdown expands and continuously

evolves to the entire 2DEG channel. Thus the local breakdown in the vicinity of the source contact precedes the breakdown on the entire 2DEG channel. If W is smaller than the minimal length, L_B, the situation is markedly different. The local breakdown should be absent at any current levels, and the cascadelike electron-hole pair excitation takes place only as the electrons traverse the Hall bar along the 2DEG channel. The evolution of the breakdown is such that it initiates on the source-contact side of the 2DEG channel and develops along the length-wise direction towards the drain-contact side, as observed by experiments.[10–12,22]

ACKNOWLEDGMENT

We thank Y. Kawaguchi and K. Hirakawa for the assistance in the measurements using a Fourier transform spectrometer. This work has been supported by Core Research for Evolutional Science and Technology (CREST) of Japan Science and Technology Corporation (JST).

[1] G. Ebert, K. von Klitzing, K. Ploog, and G. Waiman, J. Phys. C **16**, 5441 (1983).

[2] M. E. Cage, R. F. Dziuba, B. F. Field, E. R. Williams, S. M. Girvin, A. C. Gossard, D. C. Tsui, and R. J. Wagner, Phys. Rev. Lett. **51**, 1374 (1983).

[3] H. L. Stormer, A. M. Chang, D. C. Tsui, and J. C. M. Hwang, in *Proceedings of the 17th International Conference On the Physics of Semiconductors, San Francisco*, 1984, edited by by D. C. Chadi and W. A. Harrison (Springer, Berlin, 1985), p. 275.

[4] M. Yokoi, T. Olamoto, S. Kawaji, T. Goto, and T. Fukase, Physica B **249/251**, 93 (1998).

[5] J. Wakabayashi and S. Kawaji, J. Phys. Soc. Jpn. **44**, 1839 (1978).

[6] D. Dominguesz, K. von Klitzing, and K. Ploog, Metrologia **26**, 197 (1989).

[7] P. C. van Son, G. H. Kruithof, and T. M. Klapwijk, Phys. Rev. B **42**, 11 267 (1990).

[8] Y. Kawano, Y. Hisanaga, and S. Komiyama, Phys. Rev. B **59**, 12 537 (1999).

[9] S. Komiyama, T. Takamasu, S. Hiyamizu, and S. Sasa, Solid State Commun. **54**, 479 (1985).

[10] Y. Kawaguchi, F. Hayashi, S. Komiyama, T. Osada, Y. Shiraki, and R. Itoh, Jpn. J. Appl. Phys., Part 1 **34**, 4309 (1995).

[11] Y. Kawaguchi, S. Komiyama, T. Osada, and Y. Shiraki, Physica B **227**, 183 (1996).

[12] S. Komiyama and Y. Kawaguchi, Phys. Rev. Lett. **77**, 558 (1996).

[13] S. Komiyama and Y. Kawaguchi, Phys. Rev. B (to be published).

[14] S. Komiyama, Y. Kawano, and Y. Hisanaga, *Extended Abstract of 21st International Conference on IR&MM Waves* (edited by M. von Ortenberg and H. U. Mueller, Berlin, 1996); S. Komiyama, H. Hirai, O. Astafiev, Y. Kawano, T. Sawada, and T. Sakamoto (unpublished).

[15] K. Hirakawa, M. Endo, K. Yamanaka, Y. Hisanaga, and S. Komiyama, *Proceedings of 23th Internaitonal Conference on the Physics of Semiconductors* (World Scientific, Berlin, 1996), p. 2543.

[16] In Fig. 2(b), large voltage fluctuations are visible in V_{34} and V_{23} (at $I_{14} > +100\ \mu$A), which are measured with a time constant of 0.1 s. Interestingly, additional measurements show that the fluctuation in V_{34} negatively correlates with the one in V_{23} to cancel each other. The sum $V_{24}=V_{34}+V_{23}$ is therefore free from a remarkable fluctuation and the equality, $V_{14}-(h/2e^2)I_{14}=V_{34}+V_{23}$, can be confirmed in an accurate manner despite the apparently large fluctuations visible in Fig. 2(b). Understanding of the mechanism of the negatively correlated fluctuations is left for future study. Equivalent features are observed also in V_{12} and V_{23} in Fig. 3(b).

[17] N. Q. Balaban, U. Meirav, H. Shtrikman, and Y. Levinson, Phys. Rev. Lett. **71**, 1443 (1993).

[18] F. Thiele, U. Merkt, J. P. Kotthaus, G. Lommer, F. Malcher, U. Rossler, and G. Weimann, Solid State Commun. **62**, 841 (1987).

[19] W. Zawadzki, C. Chaubet, D. Dur, W. Knap, and A. Raymond, Semicond. Sci. Technol. **9**, 320 (1994).

[20] See Ref. 8 for a comprehensive discussion of the kinetics of electrons.

[21] Although a fraction of electrons enters the 2DEG at corner S_H as mentioned, we conventionally refer to corner S_L as the ''electron entry corner'' since a majority of electrons enter at this corner when $\mu_S-\mu_D \gg \hbar\omega_c/2$.

[22] I. I. Kaya, G. Nachtwei, K. von Klitzing, and K. Eberl, Phys. Rev. B **58**, R7536 (1998); Europhys. Lett. **46**, 62 (1999).

[23] D. C. Tsui, G. J. Dolan, and A. C. Gossard, Bull. Am. Phys. Soc. **28**, 365 (1983).